Total Differential Cross Section for Scattering of Protons by Helium and Argon*

D. H. Crandall
Joint Institute for Laboratory Astrophysics, University of Colorado, Boulder, Colorado 80302

R. H. McKnight
Physics Department, University of Virginia, Charlottesville, Virginia 22901

D. H. Jaecks
Behlen Laboratory of Physics, University of Nebraska, Lincoln, Nebraska 68508

(Received 10 October 1973; revised manuscript received 12 January 1973)

Measurements for the differential scattering of protons by helium and argon as a function of scattering angle and impact energy are presented for the range 3–20 keV and 1°–5° laboratory angle. The measurements are of the sum of elastic, inelastic, and charge-changing collisions. Comparison is made with two classical calculations, one employing the Bohr screening length, the other employing separate screening lengths for each electronic shell. For argon, the data are in significantly better agreement with the calculation employing separate screening lengths for each electronic shell.

I. INTRODUCTION AND THEORY

Differential scattering has been used extensively for the investigation of potential between colliding atomic and molecular systems. The angular scattering of atomic systems should be adequately described by a classical orbital calculation when (a) the de Broglie wavelength λ of the incident particle is small compared to the dimensions of the scattering field, and (b) the deflection due to collision is well defined within limits of the uncertainty principle.[1] For the present situation the smallest dimension of the scattering field can be represented by the impact parameter of the collision ρ, which is always larger than λ for the present data. The second condition gives a restriction on the scattering angle

$$\theta >> \lambda/2\pi\rho ,$$

which is also satisfied by all present data.

Such classical scattering was discussed by Bohr,[2] who introduced the potential function

$$V(r) = \frac{Z_1 Z_2 e^2}{r} e^{-r/a} , \tag{1}$$

where $Z_1 e$ and $Z_2 e$ are the nuclear charges, r is the internuclear distance, and $a = a_0/(Z_1^{2/3} + Z_2^{2/3})^{1/2}$ is the Bohr screening length, where a_0 is the radius of the first Bohr orbit. Differential cross sections have been calculated classically by employing this potential by Everhart, Stone, and Carbone,[3] and by Bingham.[4] Bingham's tables are the more detailed and have been used to obtain cross sections for comparison to the present data. The calculations are tabulated for various values of b/a, where b is the collision diameter or "head-on" collision distance, and $b = Z_1 Z_2 e^2/E$ (E is kinetic energy of relative motion). These calculations can thus be applied to a wide range of projectile-target combinations. Smith, Marchi, and Dedrick[5] have also calculated differential scattering from a screened Coulomb potential in a useful formalism without specifying the screening length.

Many variations of the exponential screening function have been proposed (for example, see Refs. 6 and 7). One of the simplest alternatives has been proposed by Smith *et al.*[8,9] A potential is used which has separate screening lengths for each shell of electronic structure. Smith *et al.*[9] adjusted screening lengths for each shell to give the best fit to data.[10,11] The screening lengths they obtained were in good agreement with the effective radius of each shell predicted by simple hydrogenic considerations connecting the screening radius with the ionization potential for that shell. Employing this shell-hydrogenic screening for the case of protons incident on an atomic target, we find for the potential

$$V(r) = \frac{e^2}{r} \sum_i \alpha_i e^{-r/c_i} , \tag{2}$$

where $\alpha_i = 2, 8, 8\ldots$ for K, L, $M\ldots$ shells, and $c_i = a_0 (I_H/I_i)^{1/2}$ with I_H the ionization potential of hydrogen and I_i the ionization potential of the respective electronic shells.

The classical expression for the deflection angle produced by collision is

$$\theta = \frac{\rho}{E} \int_\rho^\infty \frac{dV(r)}{dr} \frac{dr}{(r^2 - \rho^2)^{1/2}} , \tag{3}$$

with the assumption that the distance of closest approach, r_0, can be replaced by ρ for the lower limit of the integral (valid only for small-angle scattering). For a potential of the form $V = Z_{\text{eff}} e^2/r$ (where Z_{eff} is a constant) the integral is readily evaluated,[12] giving

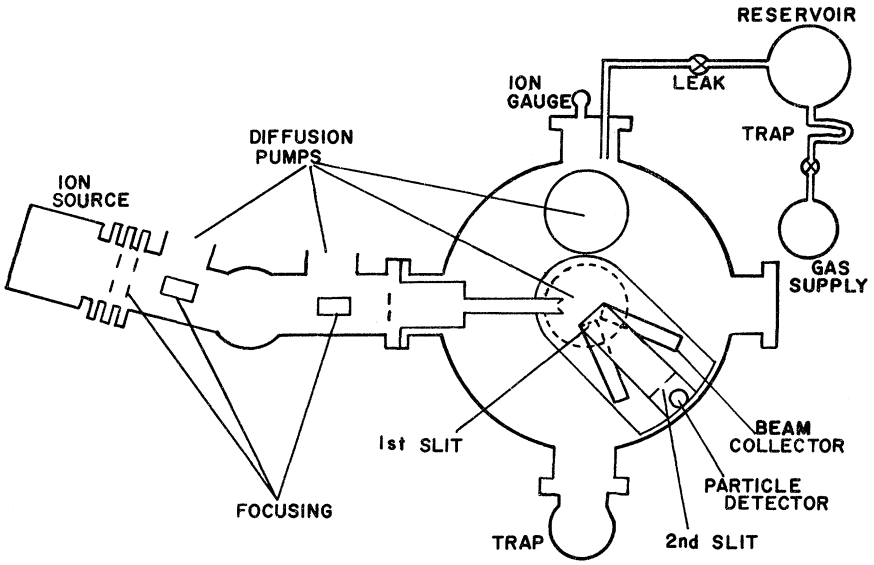

FIG. 1. General experimental schematic.

$$\theta E = Z_{\text{eff}}\, e^2/\rho \ .$$

Dose[13] has set

$$\theta E = \rho \int_{\rho}^{\infty} \frac{dV(r)}{dr} \frac{dr}{(r^2-\rho^2)^{1/2}} = \frac{Z_{\text{eff}}\, e^2}{\rho}$$

and has evaluated the integral with Smith's potential (2), thus obtaining Z_{eff}. That is, at the particular impact parameter chosen, Z_{eff} has been adjusted so that the potential $Z_{\text{eff}}\, e^2/r$ will result in classical scattering to the same angle as the multiple-screening-length potential used in evaluating the integral. The utility of Z_{eff} is that the differential scattering cross section is readily calculated from the well-known classical formula of Rutherford,

$$\frac{d\sigma}{d\Omega}(\theta) = \frac{1}{4}\left(\frac{Z_{\text{eff}}\, e^2}{2E}\right)^2 \frac{1}{\sin^4 \frac{1}{2}\theta} \ . \qquad (4)$$

Recently, Rice and Bingham[14] have undertaken another calculation of the differential scattering by employing Hartree–Fock–Slater electron probability densities to obtain the potential between colliding atomic systems as a function of the nuclear separation. This approach allows for the shell structure, assuming that the electrons remain in their unperturbed orbits during collision. Rice and Bingham compare results of their calculation with the screened-Coulomb (Bohr), the shell-screening (Smith), and available differential scattering data (including much of the present data). The potential derived using the Hartree–Fock–Slater probability densities gives differential scattering in better agreement with data than either of the other two potentials, but is generally in good agreement with the hydrogenic-shell screening results for the collision systems and range of angle and energy discussed here.

Recent literature contains other contributions of experimental and theoretical work to determine potentials for atom-atom scattering from differential scattering (for example, see Refs. 15–18). Most of this work has been carried out for slower collisions where polarization and quantum effects become important. The results presented here will be compared to the two simple classical calculations employing screened-Coulomb (Bohr) and shell-screening (Smith) potentials.

The experimental work of Taylor, Thomas, and Martin[19] demonstrates that the Bohr potential gives quite satisfactory agreement with experiment for more energetic collisions (120–830 keV) than those studied here.

II. EXPERIMENT DESCRIPTION

A. Apparatus

The apparatus, shown schematically in Fig. 1, has been discussed previously.[20,21] A more complete discussion of factors pertinent to the absolute measurement of total differential scattering cross sections will be presented here.

A beam of protons enters the scattering chamber through two 1.00-mm apertures separated by 25.9 cm. The measured width of the beam at 18.6 cm from the second aperture was 1.25 mm, indicating divergence of the proton beam to be less than $\pm 0.04^\circ$ in the scattering region.

The particle detector and scattering-angle-defining apertures are located in an externally rotatable housing. The first aperture, defining scat-

tered-particle-acceptance angle, is formed by the knife edges of two rectangular beam-collection cups. The slit formed is 0.513 mm horizontally by 31.8 mm vertically, and is located 1.63 cm from the rotation (and scattering) center. The second acceptance-geometry aperture is 12.66 cm from the first and is a rectangular hole 1.01 mm horizontally by 3.73 mm vertically. The maximum spread of acceptance angle in the horizontal plane allowed by this geometry is $\pm 1/3^\circ$. The particle detector is a bare 13-stage electron multiplier with Cu-Be dynodes mounted with the dynode string perpendicular to the beam. The entire housing assembly opens into the scattering chamber only through the first acceptance-geometry aperture. The housing is thus differentially pumped maintaining approximately $\frac{1}{100}$ of the chamber target gas pressure in the detector housing.

It should be emphasized that the construction of the apparatus was for the purpose of measuring charge transfer to the excited states H($2s$) and H($2p$) at particular impact parameters (scattering angle times energy).[20,21] In order to obtain the charge-transfer fractions, it was also necessary to measure the total scattered flux at the particular angle. The data presented here were acquired simultaneously with those of Ref. 20. The differential cross sections for scattering with charge transfer to all states of H and with charge transfer to the $2s$ or $2p$ states can be obtained by multiplying the present total differential scattering cross sections by the appropriate charge-transfer fraction from Refs. 20 or 21.

B. Quantities to be Measured

The primary quantity to be determined is the differential cross section for scattering from the target gas. For the present case we will be detecting all particles scattered by the target including those which have changed charge or have lost energy during the collision. The number of scattered particles incident on the detector is given by the relation

$$N = N_0 \rho \int_{\Delta\Omega} l \frac{d\sigma_{\text{tot}}}{d\Omega} d\Omega' , \tag{5}$$

where N_0 is the number of incident particles, ρ is the target-gas density, l is the length of the beam-target interaction region viewed by the detector, $d\sigma_{\text{tot}}/d\Omega$ is the desired differential cross section, and $\Delta\Omega$ is the solid angle of scattered-particle acceptance. If $\Delta\Omega$ is sufficiently small that $d\sigma_{\text{tot}}/d\Omega$ is nearly constant over $\Delta\Omega$, then the integral becomes $(d\sigma_{\text{tot}}/d\Omega) l\Delta\Omega$.

In terms of actually observed quantities (assuming $d\sigma_{\text{tot}}/d\Omega$ is nearly constant over $\Delta\Omega$),

$$\frac{d\sigma_{\text{tot}}}{d\Omega} = \frac{S}{\epsilon_M} \frac{e}{Q} \frac{1}{\alpha_T P} \frac{1}{(l\Delta\Omega)} , \tag{6}$$

where S is the number of detected particles (equal to $\epsilon_M N$), ϵ_M is the particle-detector efficiency, Q is the total charge passing through the scattering chamber (equal to $N_0 e$), P is the target-gas pressure, and α_T is the temperature-dependent proportionality factor between pressure and density ($\alpha_T P = \rho$). The quantities to be observed experimentally are S, Q, and P, and apparatus quantities which must be determined are ϵ_M and $l\Delta\Omega$.

C. Determination of Experiment Quantities

The quantity $l\Delta\Omega$ is a function of apertures and angle setting. As shown in Fig. 2, a portion of the beam length d is subtended by the entire area of the second aperture. However, additional parts of beam length are subtended by only a portion of the second aperture.

A simple formula for $l\Delta\Omega$ for such geometry was first given by Jordan and Brode[22]:

$$l\Delta\Omega = W_1 W_2 h_2 / YR \sin\theta$$

(quantities are as in Fig. 2). This simple formula will be least accurate at small angles θ. A more exact numerical evaluation (for a beam of negligible width) was carried out. For the present geometry the more exact evaluation agreed with the simple formula to within 1.5% at 1°. The Jordan–Brode formula has been used for data analysis.

An additional source of error in the quantity $l\Delta\Omega$ is the accuracy of angle determination. The angle setting was measured to be reproducible to better than $\pm 0.03^\circ$, but could be additionally inaccurate owing to incorrect alignment of the first defining slit on the line between the scattering center and the second defining aperture. Including the estimated accuracy of the alignment procedure, the angle accuracy is $\pm 0.05^\circ$. The alignment error is most sensitively tested by comparing the measured cross section on either side of the zero-degree position. Such a comparison is shown in Fig. 3. The discrepancy observed is slightly less than allotted by the estimated accuracy of the alignment. Owing to the symmetry, the cross section, independent of alignment, should be given by the average of the measured value left and right of zero. All other data presented were taken at angles right of zero, and corrected by a linear function constructed from the data of Fig. 3. The correction varied from 11% at 1° to 3% at 2°, and was neglected at angles above 2°.

The effect demonstrated by Fig. 3 could also arise from a nonuniform spatial distribution of protons in the finite-width beam. In this case the direct correction applied might not be appropriate, so that an uncertainty of the same order as the correction has been allowed.

Another significant error is made in the assumption that $d\sigma_{\text{tot}}/d\Omega$ is constant over $\Delta\Omega$. For the

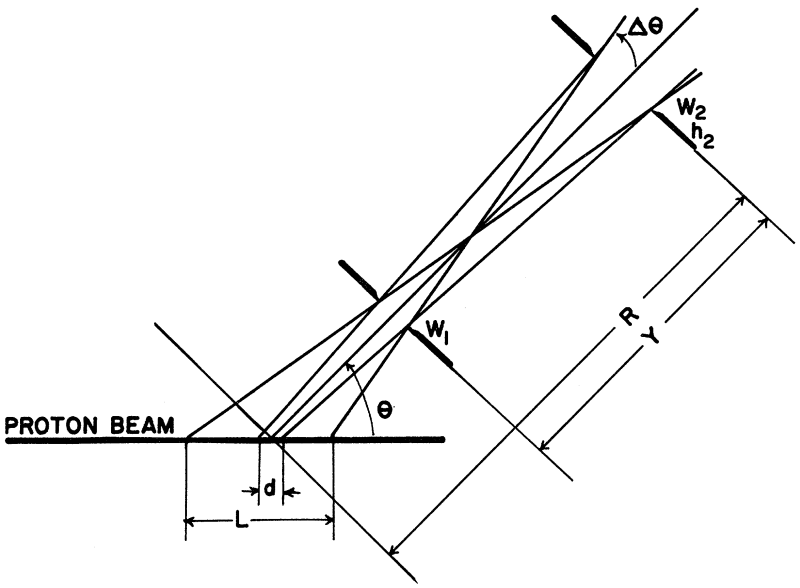

FIG. 2. Scattered-particle acceptance geometry, viewed from above.

present classical scattering, the significant variation of the expected cross section is the variation with angle, $1/\sin^4\frac{1}{2}\theta$. In order to test the error in assuming $d\sigma_{tot}/d\Omega$ constant over $\Delta\Omega$, we numerically evaluated

$$\int_{\Delta\Omega} \frac{l\,d\Omega}{\sin^4\frac{1}{2}\theta}$$

for the present geometry (but with a beam of negligible width), and compared the result with

$$\frac{1}{\sin^4\frac{1}{2}\theta}\int_{\Delta\Omega} l\,d\Omega\ .$$

The results indicate that the observed cross section may be as much as 25% higher than the true cross section at 1°, but the discrepancy reduced to about 4% by 2° and continued to reduce at higher angles.

Further, at angles less than 2.0°, part of the primary ion beam misses the beam-collection cup and thus passes through the first defining aperture into the housing. None of the primary particles can pass directly through both apertures for angles greater than 0.5° (considering beam width plus spread of acceptance angle). However, reflection of primary particles by the first slit through the second aperture was observed. This problem caused background count rates at 1° (with scattering chamber evacuated) to be as high as 15% of the signal for the case of helium target. Even though the background was measured and subtracted for each data point, some uncertainty is introduced.

In addition to the background increase, missing the beam-collection cup interferes with the measurement of Q, the total charge passing through the chamber in any trial, thus introducing additional uncertainty of about ± 5% in the measurement of this quantity.

All of the above small-angle difficulties add significantly to the error in the measured cross sections for angles less than 2.0°.

Target-gas pressure was monitored continuously

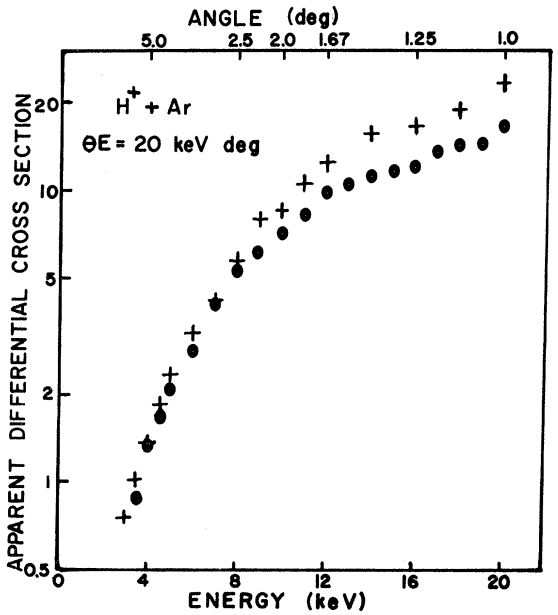

FIG. 3. Apparent differential cross section for protons on argon at $\theta E = 20$ keV deg. Scattering angles left of zero: +; scattering angles right of zero: ●.

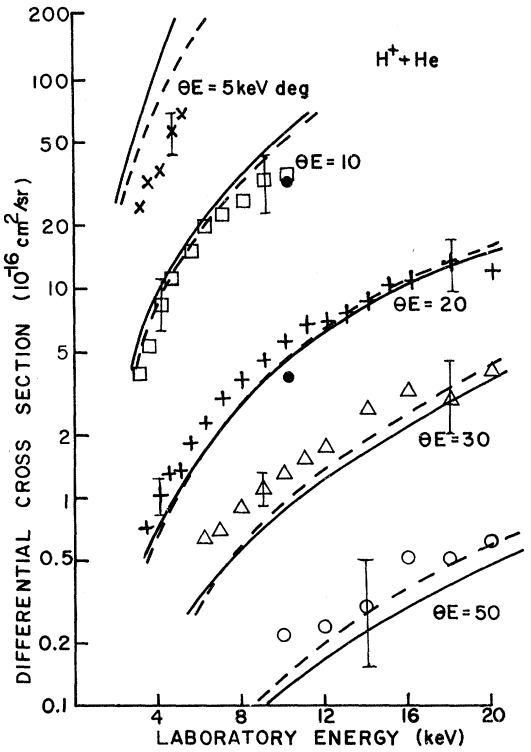

FIG. 4. Total differential scattering cross section for protons on helium. Present data: ×, □, +, Δ, ○ for impact parameters 0.45, 0.25, 0.14, 0.094, and 0.057 a.u., respectively. Data of Fitzwilson and Thomas (Ref. 27): ●. Solid curve: calculation from the work of Dose (Ref. 13). Dashed curve: calculation of Bingham (Ref. 4).

by a Bayard-Alpert-type ion gauge and was stable to 1–2% during data trials. The ion gauge was calibrated against a McLeod gauge which operated in the pressure range 1×10^{-7}–2×10^{-3} mm of Hg. The McLeod gauge was cooled with dry ice and liquid nitrogen trapped. Considerable care was taken to minimize and test for the known systematic errors associated with the McLeod gauge.[23] The residual systematic error in the McLeod gauge should not exceed ± 7% with over-all accuracy of pressures measured with the ion gauge expected to be better than ± 10%. Target-gas pressures between 2×10^{-5} and 1×10^{-3} mm of Hg were used in the experiment with linearity of signal intensity versus pressure being employed to ensure single-collision conditions. Background pressure in the scattering chamber was 1×10^{-8}–5×10^{-8} mm of Hg.

The efficiency of the bare-electron multiplier for detection of hydrogen atoms was measured directly by a unique method which has been reported.[24] The technique exploits the presence of hydrogen atoms in the 2*s* state after scattering, which can be induced to radiate 1216-Å photons by application of electrostatic fields. Such quench-induced photons were detected from the fast-scattered atoms with geometry constructed so that each atom which gave up a photon subsequently struck the first dynode of the electron multiplier. The ratio of total counted photons to coincidence count between photons and fast particles provides a direct measure of the multiplier-detection efficiency. The efficiency was assumed equal for protons and hydrogen atoms of the same velocity. This assumption has been previously used[20,25] and has been supported by experimental results.[26] The efficiency ϵ_M employed in the present data analysis contains the additional factor for transmission of pulses by the amplification scheme employed, which included discrimination. The accuracy of the values of ϵ_M used is expected to be better than ± 10%.

The sources of error in measured quantities are pressure: ± 10%; multiplier efficiency (ϵ_M): ± 10%; total incident charge: ± 5%; geometry product (Ωl): ± 2%. In addition, at small angles (less than 2°) the incident-charge uncertainty rises to about ± 10%, and the error associated with the acceptance geometry rises from a few percent to about 25%.

The reproducibility of data is expected to be primarily dependent on the reproducibility of the angle setting. The reproducibility of the data was taken to be ± 3 standard deviations of the mean of five or

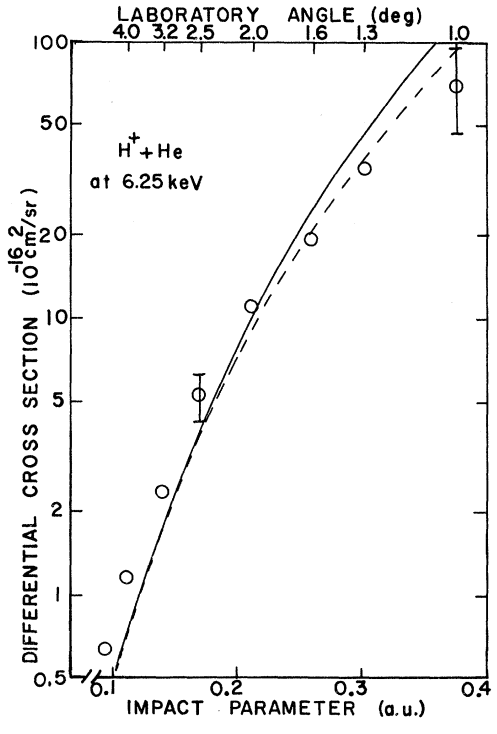

FIG. 5. Total differential scattering cross section for protons on helium at a fixed impact energy, 6.25 keV. Present data: ○. Solid curve: calculation from the work of Dose (Ref. 13). Dashed curve: calculation of Bingham (Ref. 4).

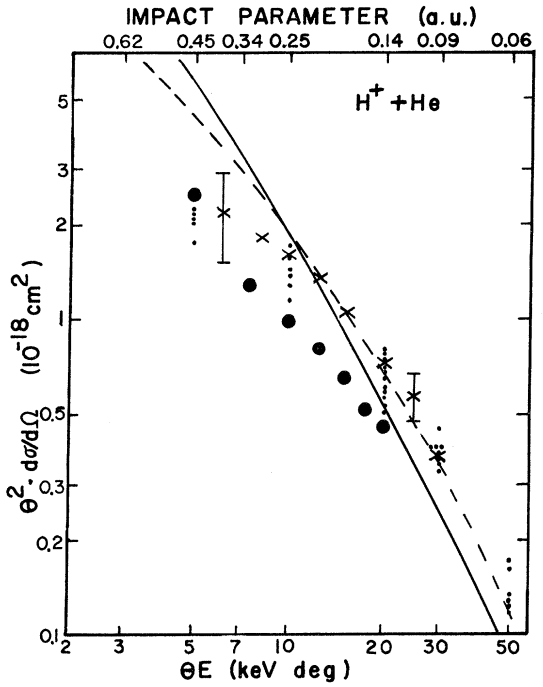

FIG. 6. Reduced differential cross sections for protons on helium. Present data at fixed θE: small dots; at 6.25 keV: ×. Data of Fitzwilson and Thomas (Ref. 27) at 10 keV:●. Solid curve: calculation from work of Dose (Ref. 13). Dashed curve: calculation of Bingham (Ref. 4).

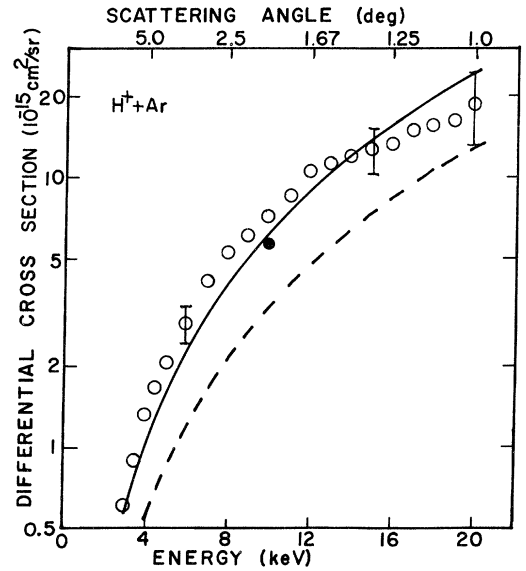

FIG. 7. Total differential scattering cross section for protons on argon at a fixed impact parameter, $\rho = 0.53$ a.u. Present data:○. Data of Fitzwilson and Thomas (Ref. 27):●. Solid curve: calculation with separate screening lengths for each electronic shell [Dose (Ref. 13)]. Dashed curve: calculation with the Bohr screening length [Bingham (Ref. 4)].

more data trials, and was typically observed to be about ±6% for angles greater than 2°, and ±12% at 1°.

The total error has been taken to be the root of the sum of the squares of the listed errors plus the square of three standard deviations. This procedure typically gives ±16% for the total error in measurements at angles greater than 2°, with the error rising to ±32% at 1°.

III. DIFFERENTIAL CROSS SECTIONS

A. Helium

The differential cross section for scattering of all particles from protons incident on helium is shown in Fig. 4, for several values of the product of incident energy and scattering angle (corresponding to particular impact parameters). Most of the data points in Fig. 4 lie closer to the Coulomb-potential results than to the hydrogenic-shell–screening-potential results. However, the difference between the two theoretical calculations is quite small and the accuracy of the data is not really sufficient to distinguish between them.

Figure 5 displays the differential cross section at a fixed incident energy as a function of impact

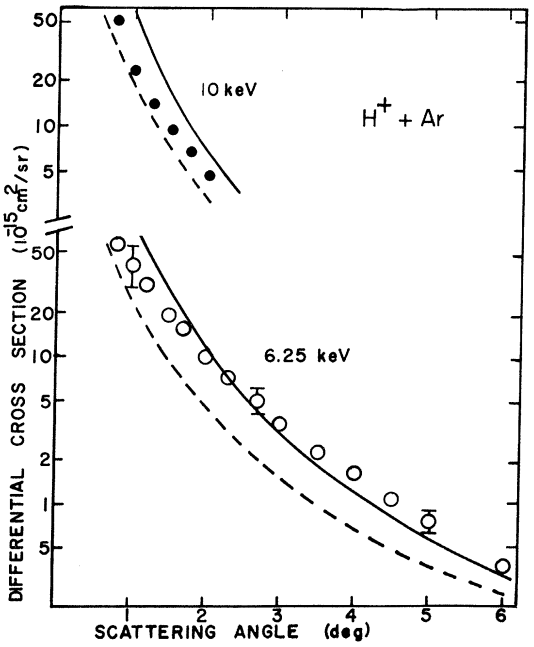

FIG. 8. Total differential scattering cross section for protons on argon at fixed energies. Present data at 6.25 keV:○. Data of Fitzwilson and Thomas (Ref. 27) at 10 keV:●. Solid curves: calculation with separate screening length for each electronic shell [Dose (Ref. 13)]. Dashed curves: calculation with the Bohr screening length [Bingham (Ref. 4)]. (Note offset between scales of 6.25 and 10 keV.)

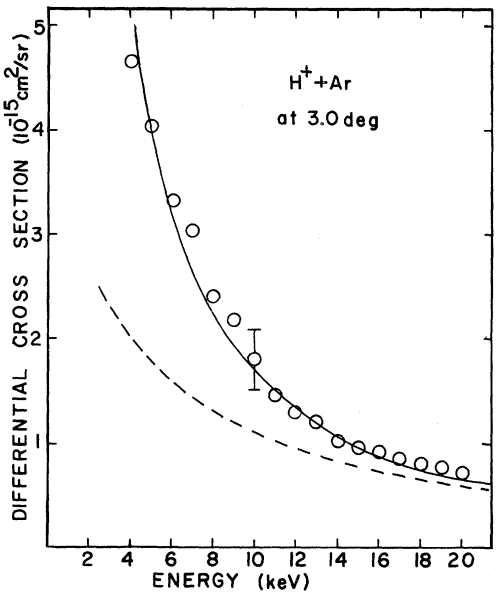

FIG. 9. Total differential scattering cross section for protons on argon at fixed scattering angle of 3°. Present work: o. Solid curve: calculation with separate screening lengths for each shell [Dose (Ref. 13)]. Dashed curve: calculation with the Bohr screening length [Bingham (Ref. 4)].

parameter. For the most distant (smallest-angle) scattering, the data begin to fall below the predicted values with the Coulomb (Bohr) potential in somewhat better agreement with the data. All quantities are for the laboratory reference frame for Figs. 4 and 5. The error bars shown represent the total error, as discussed previously.

The theoretical values for the separate electronic shell screening were obtained by substituting Dose's[13] values of Z_{eff} into the Rutherford formula (4). The theoretical curves required interpolation of the work of Bingham[4] and Dose,[13] which was accomplished graphically. The error introduced by the graphical procedure should not exceed ± 5%. The impact parameters shown in the figures are obtained from the work of Dose.[13]

Figure 6 displays all of the present data for $H^+ + He$, as well as data from Fitzwilson and Thomas[27] in the reduced cross-section representation suggested by Smith and co-workers.[5,9] The agreement between the two calculations and the data is reasonable, but with different slopes and a departure of theory and experiment for the most distant collisions. The data of Fitzwilson and Thomas are generally lower than the present data, but the discrepancy is within quoted errors (Fitzwilson and Thomas quote ± 13% systematic with ± 5% reproducibility).

In general, the theoretical results are not expected to be greatly different in the proton-helium case, since there is only one electronic shell. The similarity of the calculations, together with insufficient accuracy of the data, preclude any strong conclusion as to the superiority of any theory for this case. The calculation of Rice and Bingham[14] (not shown) gives slightly better agreement with the data than either of the calculations shown. The greatest discrepancy between the data and all of the theories is for distant collisions with the hydrogenic-shell-screening results appearing poorest. Possibly, when the electron cloud is not deeply penetrated none of the potentials employed is sufficiently accurate.

B. Argon

The absolute differential cross section for scattering of all particles from protons incident on argon is shown for the three different modes in which the data were taken: for a fixed impact parameter (Fig. 7), for fixed collision energy (Fig. 8), and for a fixed scattering angle (Fig. 9). In argon there are separate electronic shells, and the theoretical predictions are significantly different. In the range of collisions tested by the present data, the calculation employing separate hydrogenic-screening lengths for each shell is in significantly better agreement with the data.

While the absolute values of experiment and the shell-screening calculation agree well for most of the range tested, the theory and experiment depart abruptly for distant collisions. In Fig. 10, showing all of the data, the departure is seen to occur at an

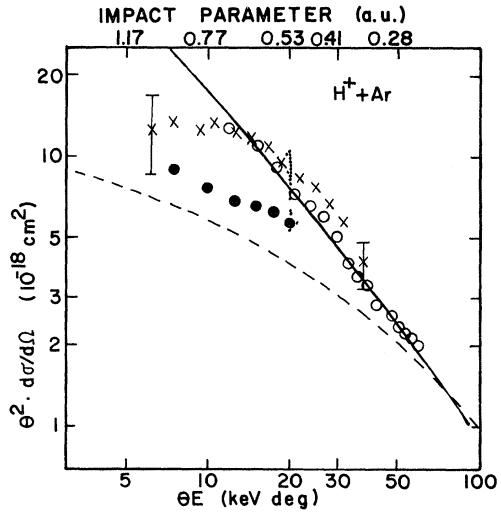

FIG. 10. Reduced differential cross section for scattering of protons by argon. Present data for $\theta E = 20$ keV deg: small dots; at 6.25 keV: ×, at 3°: ○. Data of Fitzwilson and Thomas (Ref. 27) at 10 keV: ●. Solid curve: calculation with separate screening lengths for each shell [Dose (Ref. 13)]. Dashed curve: calculation with the Bohr screening length [Bingham (Ref. 4)].

impact parameter of about 0.7 a.u. The 6.25-keV data of Fig. 8 show the departure at approximately 2° corresponding to this same impact parameter. The data of Fig. 9 do not extend to sufficiently distant collisions (low energies) to show the departure, with the result that the agreement between the data and the shell-screening calculation is excellent for the range shown in Fig. 9. The failure of the shell-screening calculation for distant collisions is similar to that indicated in the helium case, but more dramatic for argon. The data of Fitzwilson and Thomas show the same trend away from the shell-screening calculation for distant collisions, but lie lower than the present results and thus do not show clear agreement with either theory.

The calculation of Rice and Bingham[14] (not shown) provides some improvement in the distant collision range, but over the range tested it gives results similar to the hydrogenic-shell-screening results and the accuracy of the data is not sufficient to distinguish between these two theories.

For sufficiently close collisions the theories and the data apparently come into good agreement. Other data[19] for closer collisions have shown excellent agreement with the screened-Coulomb (Bohr) results.

The suggestion of this work is that in the limited range tested, the shell-screening potential is significantly better than the Coulomb screening (Bohr) in predicting the absolute value of total differential scattering cross sections for systems that have more than one electronic shell. For the most distant collisions observed, this agreement fails, with some indication that the Coulomb (Bohr) potential begins to give better agreement. However, the data available do not conclusively determine whether the Coulomb (Bohr) potential will give significantly better results for more distant collisions. The relative shapes of the theories and data in both the helium and argon cases indicate both theories rising faster than the data, but with the Coulomb (Bohr) potential having a shape somewhat closer to the experimental results.

---

*Work supported by the National Science Foundation.

[1]N. F. Mott and H. S. W. Massey, *The Theory of Atomic Collisions,* 3rd ed. (Oxford U.P., London, 1965), Chap. V, Secs. 5 and 6.

[2]N. Bohr, K. Dan. Vidensk. Selsk. Mat.-Fys. Medd. **18,** 8 (1948).

[3]E. Everhart, G. Stone, and R. J. Carbone, Phys. Rev. **99,** 1287 (1955).

[4]F. W. Bingham, J. Chem. Phys. **46,** 2003 (1967).

[5]F. T. Smith, R. P. Marchi, and K. G. Dedrick, Phys. Rev. **150,** 79 (1966).

[6]O. B. Firsov, Zh. Eksp. Teor. Fiz. **34,** 447 (1958) [Sov. Phys.-JETP **7,** 308 (1958)].

[7]C. A. Rouse, Phys. Rev. A **4,** 90 (1971).

[8]F. T. Smith, *Fifth International Conference on the Physics of Electronic and Atomic Collisions: Abstracts of Papers* (Nauka, Leningrad, 1967), p. 181.

[9]F. T. Smith, R. P. Marchi, W. Aberth, D. C. Lorents, and O. Heinz, Phys. Rev. **161,** 31 (1967).

[10]W. Aberth and D. C. Lorents, Phys. Rev. **144,** 109 (1966).

[11]P. R. Jones, F. P. Ziemba, H. A. Moses, and E. Everhart, Phys. Rev. **113,** 182 (1959); E. N. Fuls, P. R. Jones, F. P. Ziemba, and E. Everhart, Phys. Rev. **107,** 704 (1957).

[12]L. D. Landau and E. M. Lishitz, *Mechanics* (Addison-Wesley, Reading, Mass., 1960), Chap. IV.

[13]V. Dose, Helv. Phys. Acta **41,** 261 (1968).

[14]J. K. Rice and F. W. Bingham, Phys. Rev. A **5,** 2134 (1972).

[15]F. T. Smith, H. H. Fleischmann, and R. A. Young, Phys. Rev. A **2,** 379 (1970).

[16]J. Baudon, M. Barat, and M. Abignoli, J. Phys. B **3,** 207 (1970).

[17]R. L. Champion, L. D. Doverspike, W. G. Rich, and S. M. Bobbio, Phys. Rev. A **2,** 2327 (1970); W. G. Rich, S. M. Bobbio, R. L. Champion, and L. D. Doverspike, Phys. Rev. A **4,** 2253 (1971).

[18]H. F. Helbig, D. G. Millis, and L. W. Todd, Phys. Rev. A **2,** 771 (1970).

[19]G. O. Taylor, E. W. Thomas, and D. W. Martin, Phys. Rev. A **2,** 1785 (1970).

[20]D. H. Crandall and D. H. Jaecks, Phys. Rev. A **4,** 2271 (1971).

[21]R. H. McKnight and D. H. Jaecks, Phys. Rev. A **4,** 2281 (1971).

[22]E. B. Jordan and R. B. Brode, Phys. Rev. **43,** 112 (1933).

[23]P. Carr, Vacuum **14,** 37 (1964).

[24]R. H. McKnight, D. H. Crandall, and D. H. Jaecks, Rev. Sci. Instrum. **41,** 1282 (1970).

[25]F. P. Ziemba, G. J. Lockwood, and E. Everhart, Phys. Rev. **118,** 1552 (1960).

[26]B. L. Schram, H. J. H. Boerboom, W. Kleine, and J. Kistemaker, Physica (The Hague) **32,** 749 (1965).

[27]R. L. Fitzwilson and E. W. Thomas, Rev. Sci. Instrum. **42,** 1864 (1971).